

Research Article

The Antimelanogenic Activity of the Extract of Heukharang Lettuce (*Lactuca sativa* L.) Leaf

Heejin Ko ¹, Yu Jin Shon,¹ Wonchul Lim ², Tae-Gyu Nam,³ Wook Chul Kim,⁴ Nam Hee Kim ⁵, and Tae-Gyu Lim ^{1,2}

¹Department of Food Science & Biotechnology, Sejong University, Seoul 05006, Republic of Korea

²Department of Food Science & Biotechnology, and Carbohydrate Bioproduct Research Center, Sejong University, Seoul 05006, Republic of Korea

³Major of Food Science and Biotechnology, Division of Bio-Convergence, Kyonggi University, Suwon 16227, Republic of Korea

⁴Department of Medical Science, Soonchunhyang University, Asan 31538, Republic of Korea

⁵N Kim Lab, DAESAN Inc, Gangneung Science & Industry Promotion Agency, Gangneung-si, Gangwon 25440, Republic of Korea

Correspondence should be addressed to Nam Hee Kim; nkimlab.rnd@gmail.com and Tae-Gyu Lim; tglim@sejong.ac.kr

Received 19 November 2023; Revised 16 January 2024; Accepted 19 January 2024; Published 2 February 2024

Academic Editor: Ignazio Restivo

Copyright © 2024 Heejin Ko et al. This is an open access article distributed under the Creative Commons Attribution License, which permits unrestricted use, distribution, and reproduction in any medium, provided the original work is properly cited.

Heukharang (*Lactuca sativa* L.), the artificially developed lettuce cultivar for enhancement of lactucin content, exhibits antioxidant activities and sleep-promoting effects. However, potential of Heukharang as a raw material for the skin-whitening agent has not been investigated yet. This study evaluated the effects of Heukharang extract (HHE) on α -melanocyte-stimulating hormone (α -MSH)-induced melanogenesis *in vitro* and *in vivo* models. Our findings revealed that HHE (25–100 μ g/mL) effectively inhibited α -MSH-induced melanin synthesis in both 2D and 3D cell culture environments without compromising the viability of the B16F10 murine melanoma cell line. Furthermore, HHE suppressed intracellular tyrosinase activity, along with both gene and protein expression of tyrosinase (TYR) and tyrosinase-related protein (TRP)-1 and TRP-2. HHE downregulated the mRNA level of microphthalmia-associated transcription factor (*MITF*) and the phosphorylation of cAMP response element-binding (CREB) protein. The antimelanogenic activity of HHE (50 and 100 μ g/mL) was also confirmed using a zebrafish embryo model, highlighting its efficacy in inhibiting α -MSH-induced melanogenesis through the downregulating CREB/MITF/TYR signaling pathways. Moreover, our study demonstrated that a corresponding amount of lactucin (5–20 μ M) to the HHE inhibited and regulated melanogenesis. These results collectively suggest that HHE, enriched with lactucin, holds promise as a potential skin-whitening agent for nutraceutical industries.

1. Introduction

The skin, constituting 16% of the total body weight, stands as the largest organ in the human body. Its vitality and aesthetics play a significant role in enhancing the overall quality of human life. Uniform skin color is one of the critical factors in determining skin health, but hyperpigmentation which is darkened patches or spots on the skin related to melanin synthesis can cause discomfort; thus, several researchers have tried to find out novel substances or agents inhibiting pigmentation of skin cells [1, 2]. The color of the skin is determined by the synthesis and

distribution of melanin, a pigment produced through the process of melanogenesis. This intricate biological mechanism involves epigenetic regulation, where melanin is synthesized within melanocytes and subsequently transported to keratinocytes. The orchestration of multiple genes and signaling pathways is integral to the melanogenesis process [3]. Thus, hyperpigmentation can be alleviated by controlling or regulating the process of melanin synthesis and transport in various ways, and an omnidirectional molecular investigation is required to determine whether specific materials are effective for skin whitening or not [4, 5].

Tyrosinase (TYR) is a crucial enzyme for melanin synthesis, initializing melanogenesis by catalyzing the hydroxylation of tyrosine and the oxidation of L-3,4-dihydroxyphenylalanine (L-DOPA) to o-dopaquinone. This o-dopaquinone serves as a primary substrate for the subsequent synthesis of melanin [2]. The tyrosinase family genes, including TYR, tyrosinase-related protein 1 (TRP-1), and 2 (TRP-2) [6], are regulated by microphthalmia-associated transcription factor (MITF) [7, 8], which plays a key regulatory role in melanin synthesis. Especially in an eumelanogenesis pathway, both 2-carboxy-2,3-dihydroindole-5,6-quinone (L-DOPA chome) and TRP-1 were involved, generating eumelanin [9, 10]. In addition, α -melanocyte-stimulating hormone (α -MSH) is produced by keratinocytes in response to UV exposure [11]. α -MSH plays a role in elevating intracellular cyclic adenosine monophosphate (cAMP) levels and activating protein kinase A (PKA) [12, 13]. A cAMP response element-binding (CREB) protein can be activated by the cAMP/PKA signaling pathway that can phosphorylate CREB at serine¹³³ (p-CREB), finally promoting melanogenesis (PKA/CREB pathway) [14, 15]. Upon activation, the CREB protein can directly bind to the MITF promoter region, thereby stimulating MITF transcription [16]. MITF, in turn, governs the expression of numerous pigmentation genes, playing a crucial role in promoting melanocyte differentiation [17]. Thus, the interaction between these series of molecular biological and biochemical factors was collectively referred to as cAMP/PKA/CREB/MITF cascade [14].

On the other hand, lettuce (*Lactuca sativa* L.) enjoys widespread cultivation and global popularity, with significant consumption in regions such as China, the United States, and Western Europe. Its nutrition composition varied depending on the lettuce type, but all of them contain an abundance of moisture (~95%) [18]. Lettuce exhibits a diverse range of varieties distinguished by colors, sizes, and shapes. Within each type, further subdivisions into subtypes are possible, characterized by shared morphological and genetic similarities. However, the extensive genetic and morphological diversity of lettuce has led to the absence of a standardized classification system for this versatile plant. Instead, Mou [19] proposed a classification system comprising six primary lettuce types, categorized based on distinct characteristics such as head formation, leaf shape, size, stem type, and texture as follows: butterhead lettuce, crisphead lettuce, Latin lettuce, leaf or cutting lettuce, romaine or cos lettuce, and stem or stalk lettuce. A cultivar is a variety selected for desirable traits for cultivation, and several researchers have tried to select a pure line for their own purposes: higher yield, appearances [20], heat resistance [21], etc.

In Korea, Jang et al. [22] have collected and selected specific cultivars from native seeds based on their traits and productivity from 2011 to 2015 to develop a new Korean lettuce variety which has excellent functional component contents and good texture. They successfully developed

a specific and novel type of lettuce named Heukharang, which was characterized by its more pungent, bitter taste, higher hardness, black-red leaf color, even distribution of anthocyanin color throughout the leaves, and substantially higher level of lactucin ($C_{15}H_{16}O_5$, MW = 276.28 g/mol) exceeding those found in the typical lettuce, red skirt, by more than 100 times. Due to the improvement in lactucin content, several researchers have been interested in the potential use of Heukharang for developing food and/or health functional food products. Consequently, investigations into its physiological and/or biochemical effects have been conducted, encompassing areas such as antioxidant activities [22] and sleep-promoting effects [23]. Lactucin, the target compound where the Korean researchers artificially promoted its content in Heukharang, is a sesquiterpene lactone, and it has attracted attention owing to its multiple biological activities, including antimalarial [24], antihyperalgesic and anti-abiogetic [25], antiandrostene metabolism [26], and anticancer [27]. However, the effect of Heukharang and/or lactucin on skin cells has not been reported. This study examined whether Heukharang extract (HHE) and its bioactive compound lactucin would affect melanogenesis and explored the potential use of HHE as a skin-whitening agent in the nutraceutical industry. The expression of TYR, TRP-1, TRP-2, and cAMP/PKA/CREB/MITF cascade was also investigated to elucidate how the HHE treatment on skin cells contributes to regulating melanogenesis, and the antimelanogenic effect of the HHE treatment was confirmed *in vivo* using a zebrafish embryo model.

2. Materials and Methods

2.1. Reagents and Antibodies. Heukharang lettuce freeze-dried powder was purchased from HJ Biotech (Yeonggwang, Republic of Korea). The MTS reagent (3-(4,5-dimethylthiazol-2-yl)-5-(3-carboxymethoxyphenyl)-2-(4-sulfophenyl)-2H-tetrazolium) was obtained from Promega (Madison, WI, USA). Arbutin, α -melanocyte-stimulating hormone (α -MSH), dimethylsulfoxide (DMSO), lactucin, L-DOPA, and phenazine methosulfate (PMS) were obtained from Sigma (St. Louis, MO, USA). Tyrosinase (TYR) and TYR-related protein (TRP)-2 antibodies were acquired from Abcam (Cambridge, UK). TRP-1 and CREB protein 1 (CREB-1) antibodies were obtained from Santa Cruz (Dallas, TX, USA). The vinculin antibody was bought from Invitrogen (Waltham, MA, USA), and the phosphorylated CREB (p-CREB) antibody was acquired from Cell Signaling (Danvers, MA, USA).

2.2. Sample Preparation. To prepare Heukharang extract (HHE), the dried powder of Heukharang (30 g) was heated in distilled water (900 mL) and was put in a water bath (70°C, 60 rpm, 3 h). The extract solution was obtained by vacuum filtration using filter paper (Whatman, Buckinghamshire,

UK). After freeze-drying, a Heukharang water extract powder was obtained (yield of extraction = 36.53%). A stock solution of HHE (100 mg/mL) and lactucin (50 mM) was dissolved in dimethylsulfoxide (DMSO).

2.3. Cell Culture. The B16F10 cell line from murine melanoma was obtained from the Korean Cell Line Bank (Seoul, Republic of Korea). B16F10 cells were seeded and grown in Dulbecco's modified Eagle medium (DMEM) (HyClone, Logan, UT, USA) with 10% fetal bovine serum and 1% penicillin-streptomycin (Gibco, Waltham, MA, USA) at 37°C (5% CO₂).

2.4. Cell Viability Assay. The MTS assay was employed to assess the cell viability of B16F10 cells. The B16F10 cells (1×10^4) were cultured in a 96-well plate for 1 day, followed by treatment with HHE (12.5–400 µg/mL), arbutin (25–400 µg/mL), or lactucin (5–40 µM) for 72 h. After the replacement of the fresh medium, 20 µL MTS (MTS: PMS = 20:1) solution was put into individual wells. The 96-well plate containing the treated cells was incubated at 37°C with 5% CO₂. After 30 min of the incubation period, the absorbance at 490 nm was measured using a Cytation 1 microplate reader (BioTek, Winooski, VT, USA) at the Biopolymer Research Center for Advanced Material (BRCAM).

2.5. Melanin Content Assay. B16F10 cells were seeded at a density of 2.4×10^5 cells per 60 mm dish and treated with HHE (25–100 µg/mL) for 60 min prior to α -MSH treatment. The cells were treated with 100 nM of α -MSH and incubated at 37°C for 72 h. A three-dimensional melanoma cell culture system was conducted by the forced-floating method [28, 29] with slight modifications. 1×10^4 cells were cultured in an ultra-low attachment (ULA) 96-well round plate (SPL, Seongnam, Republic of Korea) at 37°C. Next day, the cells were cotreated by 100 nM α -MSH, HHE (25–100 µg/mL) or lactucin (5–20 µM). A ULA plate was incubated for 3 days at 37°C. In both 2D and 3D cell cultures, 100 µL of the cultured medium was put on each well, and melanin contents were assayed at 490 nm absorbance.

2.6. Intracellular Tyrosinase Activity Assay. B16F10 cells were seeded at a density of 2.4×10^5 cells per 60 mm dish and incubated at 37°C overnight. After pretreatment with HHE or lactucin for 1 h, the cells were treated with 100 nM α -MSH (37°C for 72 h). Subsequently, the conditioned medium was discarded, and the cells were washed with PBS twice. Cell lysis was conducted using cell lysis buffer (Cell signaling Technology, Danvers, MA, USA), followed by centrifugation (15,000g, 10 min). The supernatant was mixed with 10 mM L-DOPA and reacted (37°C for 2 h). Quantitative protein concentrations were performed using the Pierce BCA protein assay kit (Thermo Fisher, Waltham, MA, USA). The absorbance of dopachrome was measured at 490 nm.

2.7. L-DOPA Staining Assay. The L-DOPA staining assay was conducted following the procedure outlined in prior studies [30, 31], with certain modifications. The B16F10 cells were harvested with lysis buffer, and protein extracts were mixed with 10 mM Tris-HCl buffer (pH 7.0) including 1% sodium dodecyl sulfate (SDS), without β -mercaptoethanol or heating. 8% SDS polyacrylamide gel electrophoresis (SDS-PAGE) was performed. Following electrophoresis, the gel was rinsed twice with 0.1 M sodium phosphate monobasic buffers (pH 6.8) containing 10 mM L-DOPA for 30 min each at room temperature (RT), followed by incubation in the dark at 37°C for 1 h. TYR activity was confirmed with dark color bands on the gels.

2.8. Western Blotting. Protein extracts obtained from 2.7 were used for western blotting. Protein samples were subjected to 5 min heat treatment (95°C), followed by centrifugation (15,000g for 2 min at 4°C), and subsequently separated by 8% SDS-PAGE. The gels were transferred onto polyvinylidene difluoride membranes, and these membranes were blocked with Blotting-Grade Blocker (Bio-Rad, Hercules, CA, USA) for 1 h at RT. Subsequently, the membranes were incubated overnight at 4°C with primary antibodies (diluted 1:1,000) in 1× Tris-Buffered Saline with 0.1% Tween® 20 detergent (TBST). Following incubation with horseradish peroxidase-conjugated secondary antibodies (diluted 1:5,000) for 40 min at RT, the bands were detected using a chemiluminescence reader (LuminoGraph III Lite; ATTO, Tokyo, Japan) at the Biopolymer Research Center for Advanced Material (BRCAM, Seoul, Republic of Korea). Relative band intensity was calculated by the ImageJ software program (National Institutes of Health, Bethesda, MD, USA).

2.9. Real-Time Quantitative Polymerase Chain Reaction (qPCR). B16F10 cells were cultured at a density of 2.4×10^5 cells per 60 mm dish and incubated. The cells were treated with HHE (25–100 µg/mL) for 1 h, followed by the treatment of 100 nM α -MSH for 4.5 h. Total RNA was prepared using an EcoPURE Total RNA kit (Mn, Woodbury, USA). Quantitative purified RNA concentration was performed by using a NanoDrop One^c Microvolume UV-Vis spectrophotometer (Thermo Fisher). Complementary DNA was synthesized using amfiRivert cDNA synthesis platinum master mix (GenDEPOT, TX, USA) in a 20 µL volume, comprising 800 ng of total RNA. cDNA was amplified in a CFX 96 Touch Real-Time PCR Detection system (Bio-Rad) using specific primers and AccuPower® 2X GreenStar™ qPCR Master Mix (Bioneer, Daejeon, Republic of Korea). The following primer sequences were used as follows: 5'-ATC AGC AAC TCC TGT CCA GC-3' (forward), 5'-TGC TTC AGA CTC TGT GGG GA-3' (reverse) for MITF; 5'-TCT TCA CC ATG CTT TTG TGG-3' (forward), 5'-ATA GGT GCA TTG GCT TCT GG-3' (reverse) for TYR; 5'-TGG TCT GTG AAT CCT TGG AA-3' (forward), 5'-CAT TTC CAG CTG GGT TTC TC-3' (reverse) for TRP-1; 5'-CGT GCT GAA CAA GGA ATG C-3' (forward), 5'-CGA AGG ATA TAA GGG CCA CTC-3' (reverse) for

TRP-2; and 5'-CAT CAC TGC CAC CCA GAA GAC TG-3' (forward), 5'-ATG CCA GTG AGC TTC CCG TTC AG-3' (reverse) for GAPDH.

2.10. Maintenance of Zebrafish. Adult zebrafish were housed in a 3-liter acrylic tank for a period of 24 h. The maintenance system was operated on a 14/10 h light/dark cycle, and the tank temperature was maintained at 28.5°C. Zebrafish were fed three times a day. Embryos were collected from natural spawning within 30 min by turning on the light, which induced sunrise. HHE (50 and 100 µg/mL) was treated zebrafish embryos at 8 h after fertilization. Then, the effects of the HHE treatment on the melanogenesis of zebrafish were observed under the stereomicroscope.

2.11. Measurement of Melanin Contents in Zebrafish Embryos. Protein from zebrafish embryos was extracted using zebrafish embryos using PRO-PREP™ protein extraction solution (Intron, Sungnam, Republic of Korea), followed by centrifugation for collecting the pellet. After exposing to 500 µL of 1 N NaOH (60°C for 30 min), the melanin contents in the suspension were quantified at 490 nm using a microplate reader (BioTeK, Santa Clara, CA, USA).

2.12. High-Performance Liquid Chromatography (HPLC) Analysis. Contents of lactucin in HHE were quantified using the HPLC system (Agilent Technologies, Santa Clara, CA, USA). Sample separation was used by Agilent Eclipse XDB-C18 (4.6 mm ID × 250 mm, 5 µm) at 0.8 mL/min of the flow rate. The mobile phase was applied by solvent A (0.1% formic acid in water) and B (0.1% formic acid in acetonitrile), and the gradient program is summarized in Table S1.

2.13. HPLC-High-Resolution-MS/MS Analysis. To identify lactucin in the HHE, LC-MS/MS analysis was performed by a method described in a previous study with some modifications [32]. For the HPLC analysis, an ACQUITY UPLC BEH C18 column (130 Å, 1.7 µm, 2.1 mm × 50 mm) (Waters, Milford, MA, US) was used at 45°C, and the column was equilibrated for 1 min. The mobile phase was composed of solvent A (0.1% formic acid in water) and solvent B (0.1% formic acid in acetonitrile) with 0.3 mL/min of the flow rate. Sample volume was used 10 µL to an injector, and the detection wavelength was 210 nm. HHE (200 mg/mL) and lactucin (1 µg/mL) were used for this experiment. An elution gradient program was as follows: 0–1 min, 2% B; 1–15 min, 20% B; 15–15.5 min, 90% B; 15.5–17.5 min, 90% B; and 17.5–18 min, 2% B. Mass spectrometry analysis was conducted by using an Orbitrap Exploris 120 mass spectrometer (Thermo Fisher Scientific, Hemel Hempstead, UK) with a heated electrospray ionization (H-ESI) interface (Thermo Fisher Scientific). The mass spectrometric conditions were performed as follows: spray voltage, 2500 V in negative ion mode; collision gas (nitrogen); sheath gas, 50 arbitrary unit; auxiliary gas, 10 arbitrary unit; sweep gas, 1 arbitrary unit; ion transfer tube temperature, 325°C; and vaporizer temperature, 350°C. The full-MS scan mode was detected at

120,000 resolution at m/z 100–1500 and RF Lens at 70%. Precursor ions were fragmented by higher energy collisional dissociation with a normalized collision energy of 15, 30, and 60% detected at 15,000 resolution. All data were analyzed using Freestyle software (Thermo Fisher Scientific).

2.14. Statistical Analysis. All experimental data were presented as the mean ± standard deviation. Statistical analysis was conducted using Student's *t*-test with Microsoft Excel 2019 (Redmond, WA, USA). *p* < 0.05 was accepted to show a significant difference.

3. Results

3.1. HHE Shows No Cytotoxicity and Suppresses Melanogenesis. Before testing the effect of HHE on melanogenesis, a cell viability assay was conducted to assess the potential effect of HHE on B16F10 cells. HHE demonstrated no significant cytotoxicity up to a concentration of 400 µg/mL (Figure 1(a)), compared to that of 400 µg/mL of arbutin (positive control) that showed significant cytotoxicity (Figure S1(d)). When we measured extracellular melanin contents of the HHE (25–100 µg/mL)-treated cells, induction of melanogenesis by α-MSH (100 nM) was significantly decreased in both 2D (Figure 1(b)) and 3D melanoma cell culture systems (Figure 1(c)). In a specific range of concentration (25–100 µg/mL), a dose dependency of the effect of HHE was clearly observed in a 2D culture (*p* < 0.05), and all HHE treatment groups reduced melanin contents to the similar level of the control group in a 3D culture. The plateau of the effect was also observed in a higher concentration of HHE-treated groups (100–400 µg/mL) in a 2D culture (Figure S1(e)).

3.2. HHE Reduces Intracellular TYR Activity. We applied L-DOPA, a substrate for the TYR reaction, to test the effect of HHE treatment on the intracellular TYR activity. The pretreatment of HHE significantly suppressed intracellular TYR activity (Figure 2(a)). The HHE pretreatment induced a decreased level of TYR activity, and intracellular melanogenesis induced by α-MSH was also significantly reduced as TYR activity decreases (Figure 2(b)). A dose dependency of the HHE treatment was clearly observed in both results.

3.3. HHE Inhibits and Regulates the Expression of Melanogenic Enzymes. To validate the downregulatory effect of the HHE treatment on melanogenic enzymes, protein expressions of TYR, TRP-1, and TRP-2 in the HHE-treated B16F10 cells were compared by western blotting analysis (Figure 3(a)). Figure 3(b) shows that the HHE treatment significantly decreased gene expression of the key enzymes associated with melanogenesis (TYR, TRP-1, and TRP-2). To check the effect of the HHE treatment on the upstream regulatory action of the cAMP/PKA/CREB/MITF cascade, changes in mRNA expression of *MITF* were confirmed (Figure 3(c)). We found that the HHE downregulated *MITF* expression. In addition, the

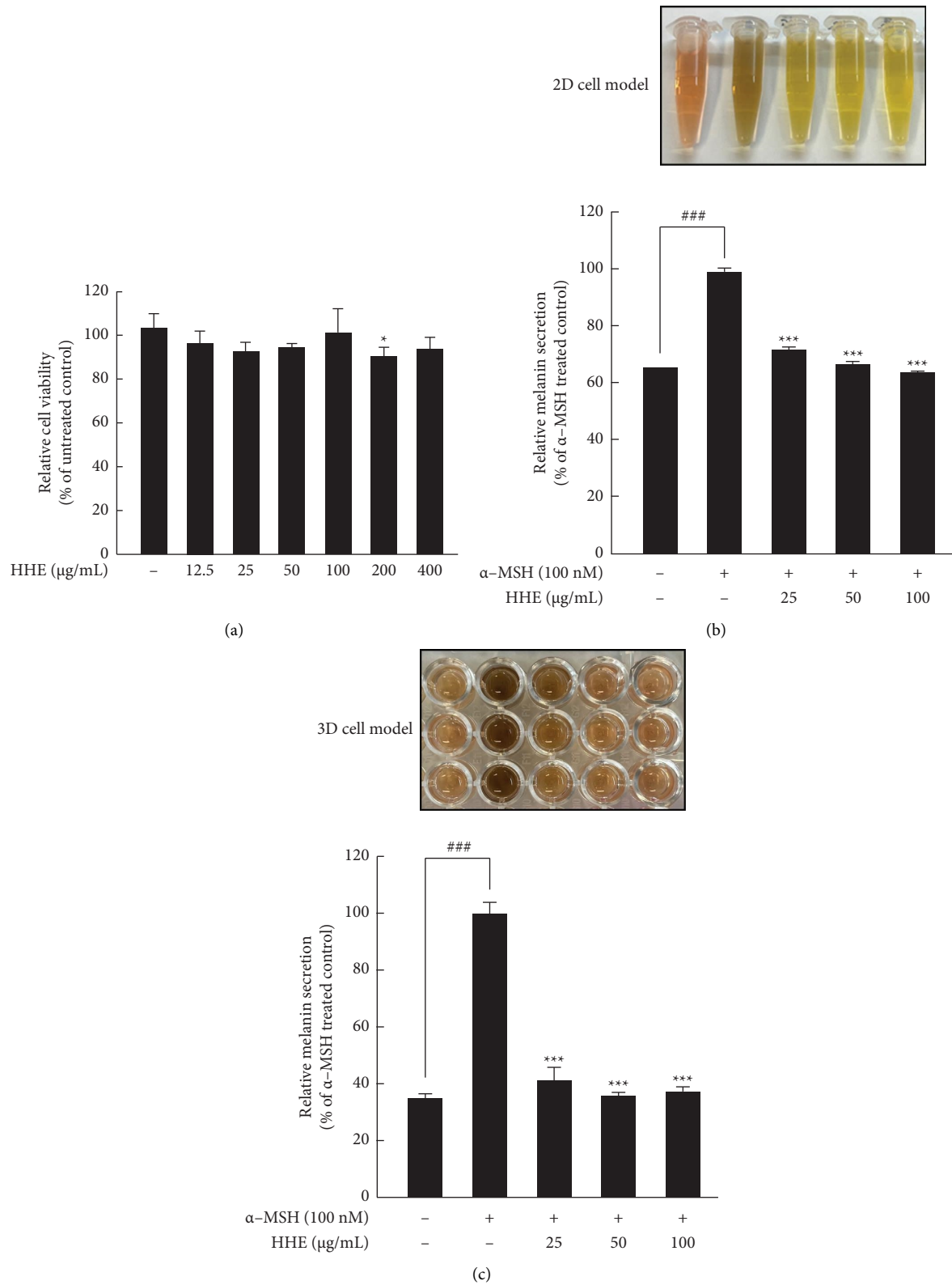


FIGURE 1: Effects of Heukharang (HHE) on cytotoxicity and melanin synthesis in B16F10 cells. (a) Cell viability of the HHE-treated B16F10 cells (* $p < 0.05$ in comparison with the untreated group). (b) Extracellular melanin contents of the 2D cell culture system. (c) Extracellular melanin contents of the 3D cell culture system (### $p < 0.001$ versus the untreated group; *** $p < 0.001$ in comparison with the α -MSH-treated group).

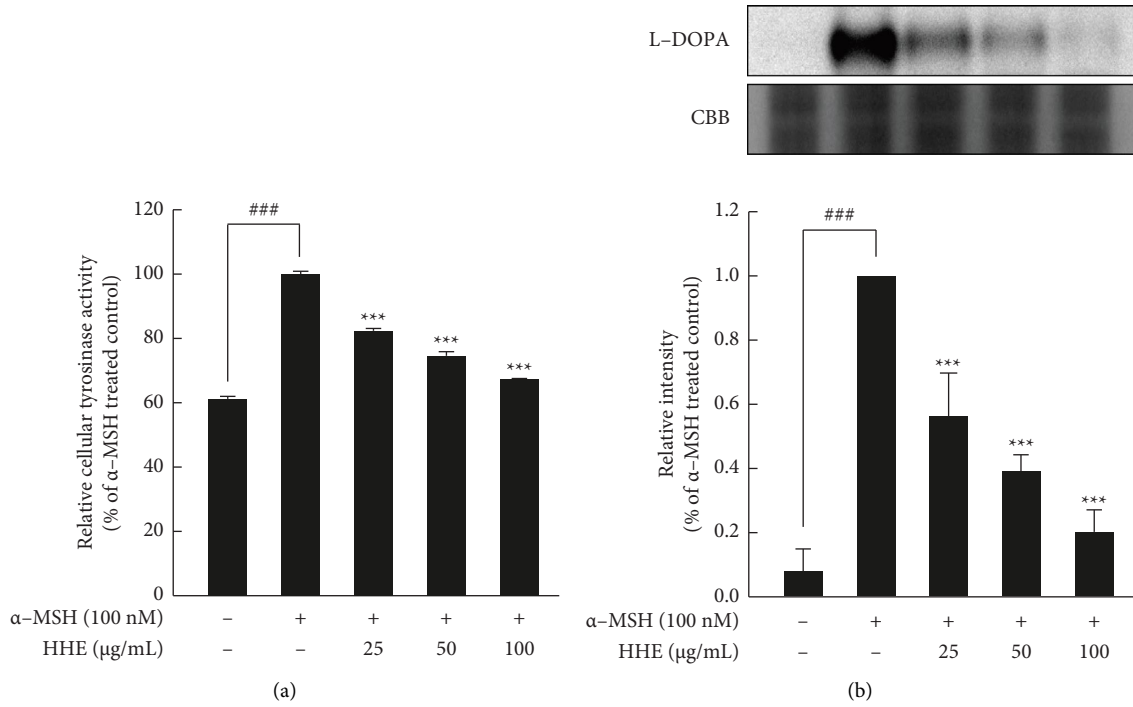


FIGURE 2: Effects of Heukharang (HHE) on intracellular tyrosinase (TYR) enzyme activity in B16F10 cells. (a) Intracellular TYR activity of the HHE-treated B16F10 cells. (b) L-DOPA staining results and intracellular melanin contents of the HHE-treated B16F10 cells (### $p < 0.001$ in comparison with the untreated group; *** $p < 0.001$ in comparison with the α-MSH-treated group).

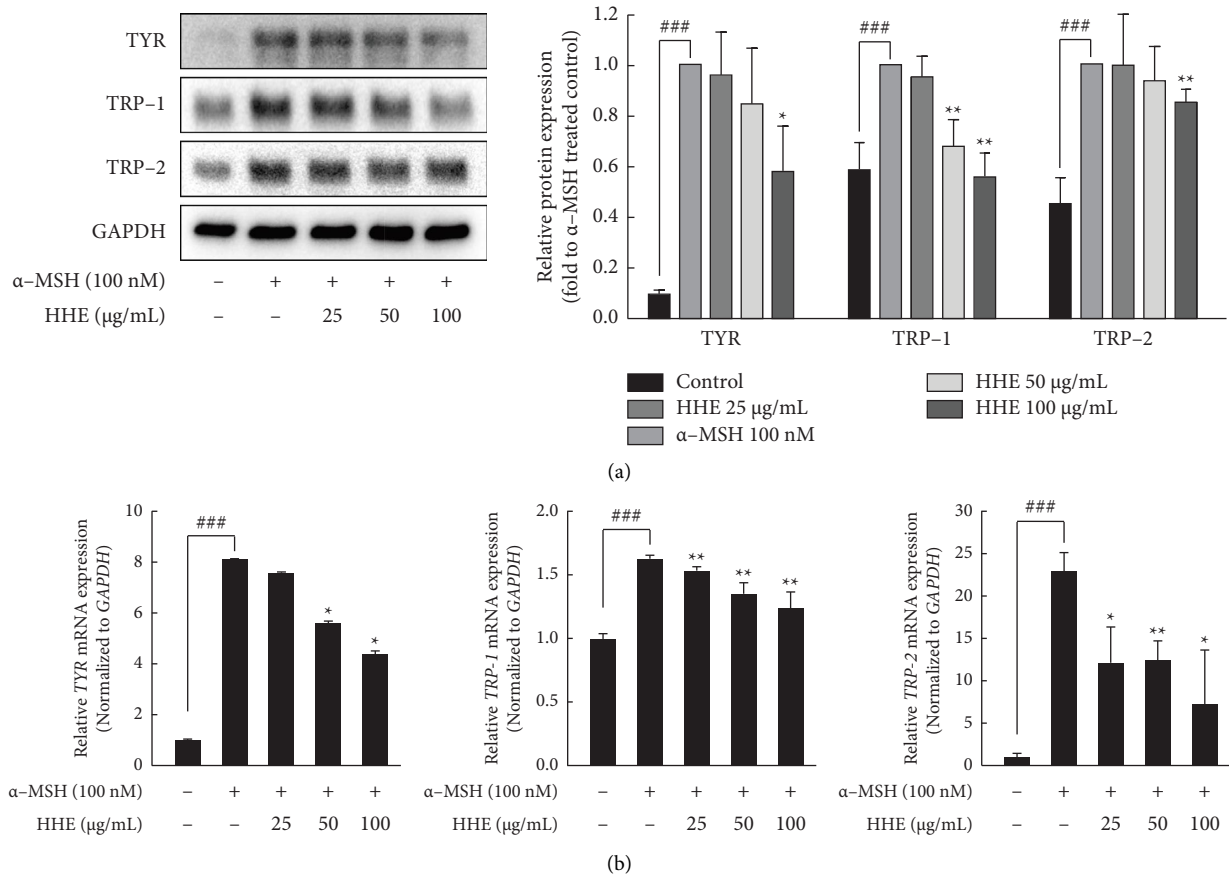


FIGURE 3: Continued.

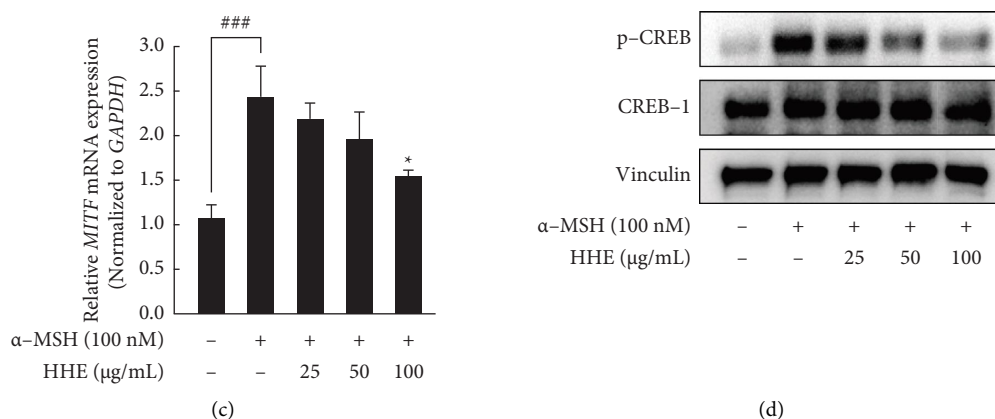


FIGURE 3: Effects of Heukharang (HHE) on the expression of melanogenic enzymes in B16F10 cells. (a) Western blotting expression of tyrosinase (TYR), tyrosinase-related protein 1 (TRP-1), and 2 (TRP-2) in the HHE-treated B16F10 cells. (b) Relative mRNA expression of *TYR*, *TRP-1*, and *TRP-2* in the HHE-treated B16F10 cells. (c) Relative mRNA expression of microphthalmia-associated transcription factor (*MITF*) in the HHE-treated B16F10 cells. (d) Western blotting analysis of phosphorylated CREB (p-CREB) and cAMP response element-binding protein 1 (CREB-1) in the HHE-treated B16F10 cells (^{###} $p < 0.001$ in comparison with the untreated group; * $p < 0.05$ and ** $p < 0.01$ in comparison with the α -MSH-treated group).

phosphorylation level of CREB was confirmed (Figure 3(d)). Expression of phosphorylated CREB was decreased by HHE treatment, dose-dependently.

3.4. HHE Inhibits Melanogenesis in Zebrafish. Figure 4(a) shows that the HHE treatment inhibited the body pigmentation of zebrafish with more than 90% of the survival and hatching rate (Figures S1(b) and S1(c), respectively). In addition, HHE treatment significantly reduced melanin contents in an embryo of zebrafish in a dose-dependent manner (Figure 4(b)).

3.5. Lactucin Is an Active Constituent of the HHE on Melanogenesis. HHE used in this study contained 0.23 mg of lactucin/g measured by HPLC analysis (Figures S2(a) and S2(b)), and the lactucin in the HHE was identified by LC-MS/MS analysis (Figures S2(b)–(d)). Figures 5(a) and 5(b) show that lactucin prepared based on the measured amount (5–20 μ M) also significantly decreased melanin secretion induced by α -MSH with a slight cytotoxicity. We confirmed that intracellular melanogenesis of B16F10 cells was also significantly reduced by lactucin treatment with both L-DOPA staining assay (Figure 5(c)) and western blotting expressions of TYR, TRP-1, and TRP-2 (Figure 5(d)).

4. Discussion

Heukharang which is well known for a sleep-promoting effect reported higher antioxidant activity compared with red skirt lettuce [23, 33]. Plant extracts with antioxidant activity could have potential of inhibitory effects on melanogenesis [34]. Heukharang extracts used in this study showed antioxidant activities including 8.31 ± 0.61 mg gallic

acid equivalent/g of phenolic contents, 18.81 ± 1.67 mg quercetin equivalent/g of flavonoid contents, and increasing DPPH radical scavenging activity, dose-dependently (Figure S1(a)).

This study represents the first elucidation of the potential use of HHE as an antimelanogenic agent in the nutraceutical industry. The *in situ* test was performed by exposing the *in vitro* cell culture model to the HHE treatment and then α -MSH, inducer of melanogenesis [12, 13] and/or substrate (L-DOPA) of key melanogenic enzyme action [35]. The skin-whitening effect of the HHE at an *in vivo* level was also confirmed using one of the animal alternative test methods, the zebrafish model.

Indeed, pretreatment of the HHE only for 1 h greatly inhibited α -MSH-induced melanogenesis without affecting cell viability of the B16F10 cells, more than 90% of the cells remained viable even after 72 h of exposure to HHE at concentrations up to 400 μ g/mL. This study employed the melanocyte aggregates as an alternative to the artificial skin model, bridging the experimental gap between 2D cell culture systems and animal models [29]. Notably, pretreatment with HHE (25–100 μ g/mL) effectively inhibited α -MSH (100 nM)-induced melanin synthesis in both the 2D and 3D culture systems, as illustrated in Figures 1(b) and 1(c). In comparison of the experimental results reported in the previous study [36], which treated 50 μ g/mL of arbutin, a well-known melanogenesis inhibitor in cosmetics and medicines, on 100 nM of α -MSH-stimulated B16F10 cells, the HHE applied in this study indicated a remarkable reduction effect on melanin synthesis (Figure S1(e)).

When intracellular responses of the cells to the HHE pretreatment were observed, increased conversion L-DOPA to L-DOPA chrome induced by α -MSH in eumelanogenesis was successfully suppressed. The HHE decreased TYR

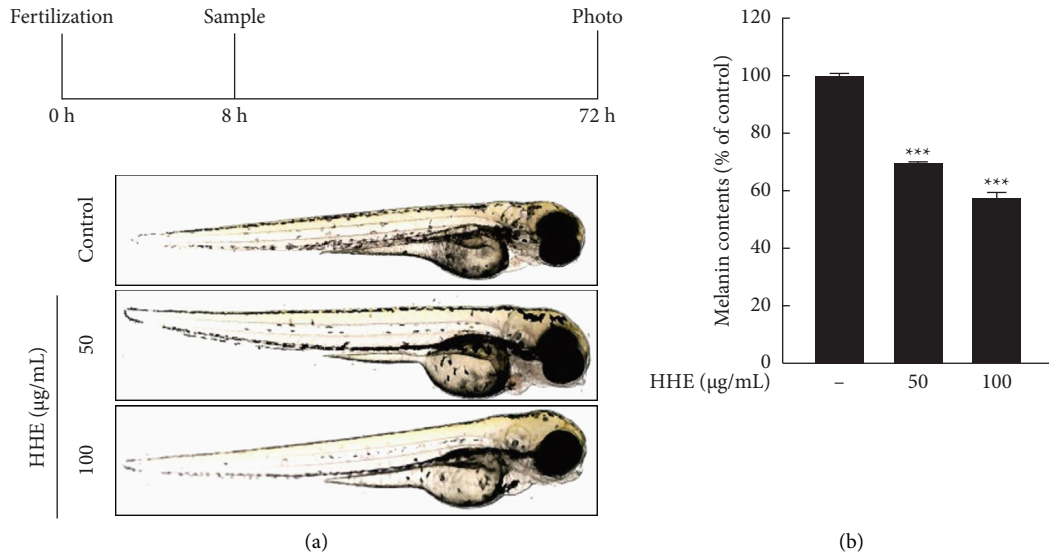


FIGURE 4: Effects of Heukharang (HHE) on melanogenesis in zebrafish. (a) Stereomicroscopic image of the HHE-treated zebrafish. (b) Melanin retention of the HHE-treated zebrafish embryos (***p* < 0.001 in comparison with the untreated group).

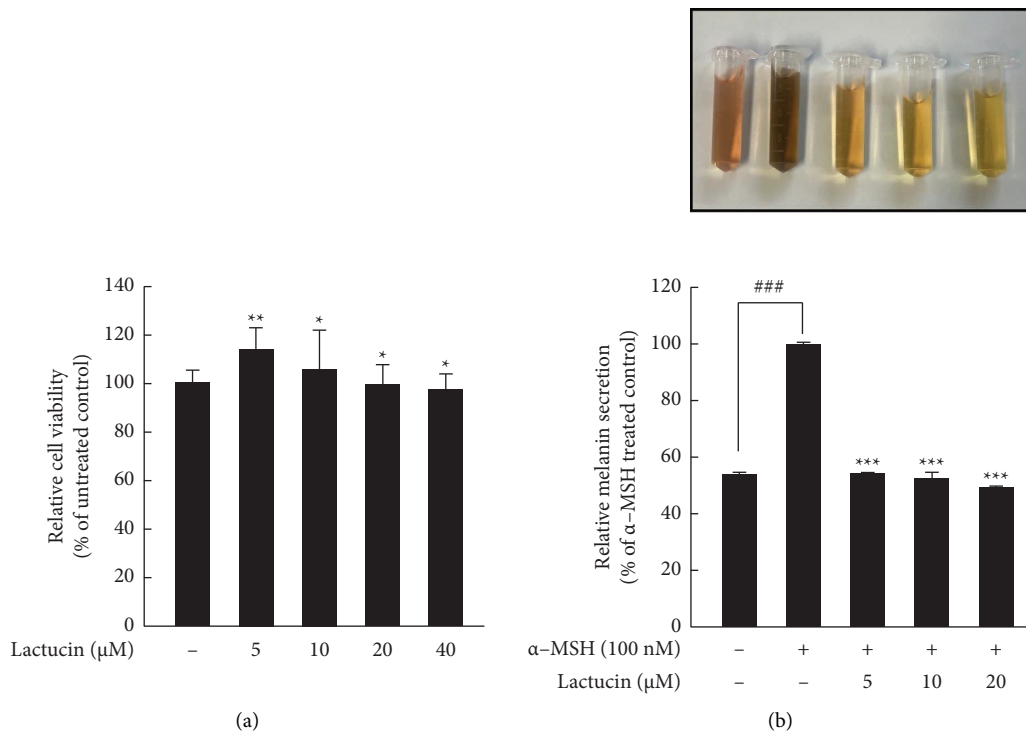


FIGURE 5: Continued.

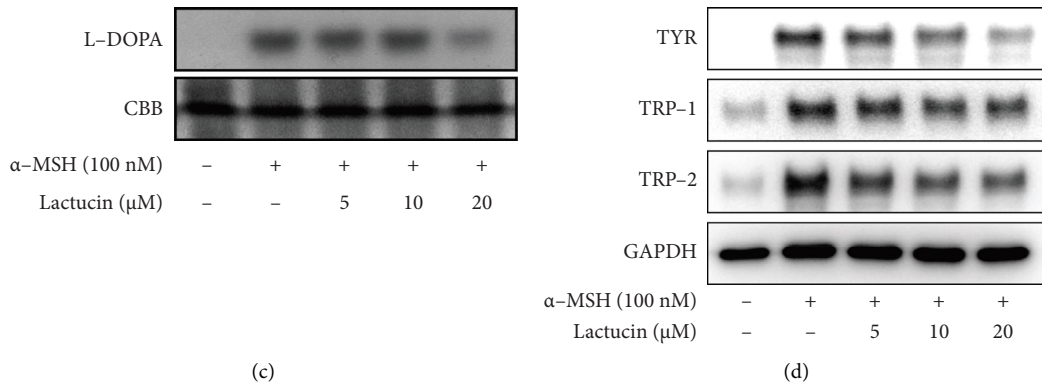


FIGURE 5: Effects of lactucin on melanogenesis in B16F10 cells. (a) Cell viability of lactucin-treated B16F10 cells. (b) Extracellular melanin contents of lactucin-treated B16F10 cells (* $p < 0.05$ and ** $p < 0.01$ in comparison with the untreated group). (c) L-DOPA staining results of lactucin-treated B16F10 cells (### $p < 0.001$ versus untreated group; *** $p < 0.001$ in comparison with the α -MSH-treated group). (d) Western blotting analysis of tyrosinase (TYR), tyrosinase-related protein 1 (TRP-1), and 2 (TRP-2) in B16F10 cells treated with lactucin.

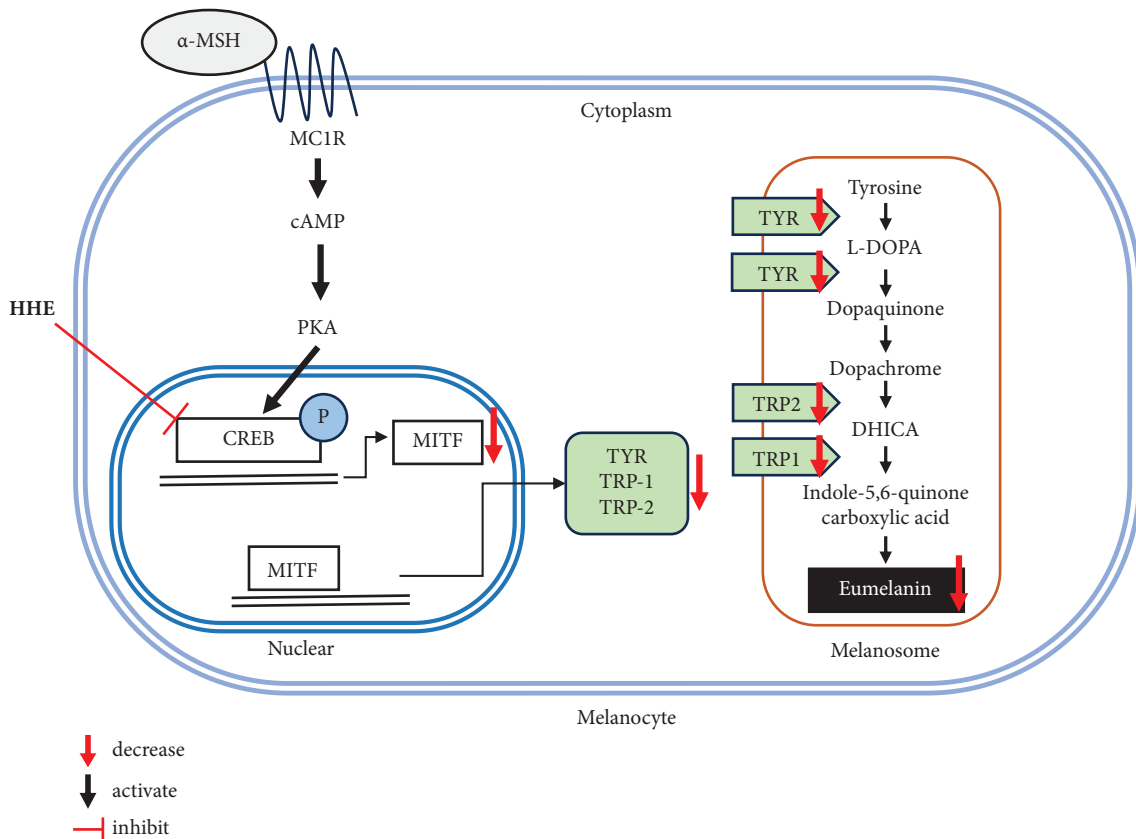


FIGURE 6: Schematic diagram of α -MSH-induced melanogenesis. HHE downregulates the CREB/MITF signaling pathway, leading to subsequent reduction in the expression of melanogenic proteins (TYR, TRP-1, and TRP-2) and melanin synthesis.

enzyme activity (Figure 2(a)) and also significantly reduced the production of dopachrome from L-DOPA, also called tyrosinase zymography. Protein expression of TYR is also significantly suppressed by the HHE treatment (Figure 3). TYR activity is crucial to melanogenesis [13]; thus, inhibition of enzymatic activity and/or expression of TYR by the HHE treatment exert a significant influence on the overall pathway of melanogenesis. In addition, the

pretreatment of HHE exhibited a dose-dependent impact on the relative expressions of TRP-1 and TRP-2. Notably, our result showed that changes in TRP-1 expression were more noticeable than in TRP-2 (Figure 3(a)). In an eumelanogenesis pathway, TRP-1 oxidizes 5,6-dihydroxyindole-2-carboxylic acid (DHICA) to a carboxylated indolequinone, a precursor that is ultimately transformed into eumelanin. On the other hand, TRP-2 catalyzes the rearrangement of

dopachrome to DHICA [37]. It is assumed that pretreatment of HHE inhibits melanin synthesis by suppressing TYR itself and preventing reorganization L-DOPA chrome and oxidizing DHICA to an eumelanin precursor.

The process of melanin synthesis is very complex and involves a number of molecular biological factors [13, 14]. This study considered expressions of p-CREB, CREB-1, and MITF to examine the effect of the HHE on the B16F10 cells in a cAMP/PKA/CREB/MITF cascade [14]. The results of this study show that the HHE treatment downregulates p-CREB and mRNA of *MITF*. The role of MITF as a master regulator in melanocyte development has been extensively studied and established [8, 38]. α -MSH induces the production of cAMP, and the increase in cAMP levels triggers the phosphorylation of the CREB transcription factor, subsequently facilitating MITF activation. This cascade of events positively regulates the transcription TYR, TRP-1, and TRP-2 [39–42]. Thus, this study shows that treatment of the HHE negatively regulates melanogenesis by suppressing p-CREB and MITF, which are transcription factors of key melanogenic enzymes TYR, TRP-1, and TRP-2.

Zebrafish is a valuable model system to evaluate anti-melanogenesis activity because it has similar genetic structures and organs to human beings [43]. To confirm the HHE treatment successfully control melanin synthesis without safety issue at an *in vivo* level, this study treated zebrafish with HHE (50 and 100 $\mu\text{g}/\text{mL}$). Melanogenesis in zebrafish is successfully controlled, and more than 90% of zebrafish survived and hatched. Thus, reviewing HHE as a skin-whitening agent in the nutricosmetic industry is reasonable.

5. Conclusions

This is the first report elucidating antimelanogenic activity of Heukharang and/or lactucin *in vitro* and *in vivo*. We suggest the mode of action of the HHE treatment on eumelanogenesis (Figure 6) based on scientific data demonstrating that pretreatment HHE on the skin inhibits melanin synthesis by regulating the CREB/MITF signaling pathway. In addition, lactucin, a well-known bioactive constituent in Heukharang lettuce, is one of the major active compounds in the HHE on antimelanogenesis. Therefore, HHE could be quite useful as a skin-whitening agent, preventing the abnormal accumulation of melanin in the cosmetic industry's melanogenesis process.

Data Availability

The string data that support the findings of this study are included within the article and the supplementary information. Also, the integer data used to support the findings of this study are available from the corresponding author upon request.

Conflicts of Interest

The authors declare that they have no conflicts of interest.

Authors' Contributions

H. Ko and Y. J. Shon contributed equally to this work.

Acknowledgments

This research was funded by the Ministry of Science and ICT and by the National Research Foundation of Korea (NRF) grant funded by the Korea Government (MSIT), grant no. 2020R1C1C100467011, by the Bio & Medical Technology Development Program of the National Research Foundation (NRF) funded by the Ministry of Science & ICT (NRF-2022M3A9I5082349). This research was supported by the Basic Science Research Program through the National Research Foundation of Korea (NRF), funded by the Ministry of Education (2022R1A6A1A03055869).

Supplementary Materials

Table S1: mobile phase conditions of HPLC. Figure S1: antioxidant activity of the HHE and effect of HHE treatment on survival and hatching rate of zebrafish. (a) DPPH radical scavenging activity of the HHE. (b) Survival rate (%) of the HHE-treated zebrafish. (c) Hatching rate (%) of the HHE-treated zebrafish. (d) Relative cell viability when treated with arbutin (25–400 $\mu\text{g}/\text{mL}$). (e) Comparison of relative melanin secretion of HHE (100–400 $\mu\text{g}/\text{mL}$) and arbutin (100 $\mu\text{g}/\text{mL}$). Figure S2: chromatogram of lactucin in HHE using HPLC and LC-MS/MS analysis (a) HPLC chromatogram of the HHE. (b) HPLC chromatogram of lactucin. (c) Total ion chromatogram (TIC) of HHE and lactucin. (d) Full-scan MS1 spectrum of HHE and lactucin at 10.45 min (red line of (c)). (e) Fragment ion spectrum (MS/MS) of the precursor ion of *m/z* 275.09 in the MS1 spectrum. (*Supplementary Materials*)

References

- [1] D.-U. Jo, Y.-W. Chin, Y. Kim, K.-T. Kim, T.-W. Kim, and T.-G. Lim, "By-product of Korean liquor fermented by *Saccharomyces cerevisiae* exhibits skin whitening activity," *Food Science and Biotechnology*, vol. 31, no. 5, pp. 587–596, 2022.
- [2] S. Parvez, M. Kang, H. S. Chung et al., "Survey and mechanism of skin depigmenting and lightening agents," *Phytotherapy Research*, vol. 20, no. 11, pp. 921–934, 2006.
- [3] S. Zhou, H. Zeng, J. Huang et al., "Epigenetic regulation of melanogenesis," *Ageing Research Reviews*, vol. 69, Article ID 101349, 2021.
- [4] Y. Jin, J. H. Kim, H.-D. Hong et al., "Ginsenosides Rg5 and Rk1, the skin-whitening agents in black ginseng," *Journal of Functional Foods*, vol. 45, pp. 67–74, 2018.
- [5] Y.-R. Song, W.-C. Lim, A. Han et al., "Rose petal extract (*Rosa gallica*) exerts skin whitening and anti-skin wrinkle effects," *Journal of Medicinal Food*, vol. 23, no. 8, pp. 870–878, 2020.
- [6] P.-Y. Zhu, W.-H. Yin, M.-R. Wang, Y.-Y. Dang, and X.-Y. Ye, "Andrographolide suppresses melanin synthesis through Akt/GSK3 β / β -catenin signal pathway," *Journal of Dermatological Science*, vol. 79, no. 1, pp. 74–83, 2015.
- [7] A. Kawasaki, M. Kumasaka, A. Satoh et al., "MITF contributes to melanosome distribution and melanophore dendricity," *Pigment cell and melanoma research*, vol. 21, no. 1, pp. 56–62, 2008.

- [8] C. Levy and D. E. Fisher, "Dual roles of lineage restricted transcription factors: the case of MITF in melanocytes," *Transcription*, vol. 2, no. 1, pp. 19–22, 2011.
- [9] H. Ando, H. Kondoh, M. Ichihashi, and V. J. Hearing, "Approaches to identify inhibitors of melanin biosynthesis via the quality control of tyrosinase," *Journal of Investigative Dermatology*, vol. 127, no. 4, pp. 751–761, 2007.
- [10] C. Mahendra Kumar, U. Sathisha, S. Dharmesh, A. A. Rao, and S. A. Singh, "Interaction of sesamol (3, 4-methylenedioxyphe- nol) with tyrosinase and its effect on melanin synthesis," *Biochimie*, vol. 93, no. 3, pp. 562–569, 2011.
- [11] L. Li, D.-N. Hu, H. Zhao, S. A. McCormick, J. J. Nordlund, and R. E. Boissy, "Uveal melanocytes do not respond to or express receptors for α -melanocyte-stimulating hormone," *Investigative Ophthalmology and Visual Science*, vol. 47, no. 10, pp. 4507–4512, 2006.
- [12] S. Corre, A. Primot, E. Sviderskaya et al., "UV-induced expression of key component of the tanning process, the POMC and MC1R genes, is dependent on the p-38-activated upstream stimulating factor-1 (USF-1)," *Journal of Biological Chemistry*, vol. 279, no. 49, pp. 51226–51233, 2004.
- [13] Z. Rzepka, E. Buszman, A. Beberok, and D. Wrzeński, "From tyrosine to melanin: signaling pathways and factors regulating melanogenesis," *Postępy Higieny i Medycyny Doświadczalnej*, vol. 70, pp. 695–708, 2016.
- [14] T. Fu, B. Chai, Y. Shi, Y. Dang, and X. Ye, "Fargesin inhibits melanin synthesis in murine malignant and immortalized melanocytes by regulating PKA/CREB and P38/MAPK signaling pathways," *Journal of Dermatological Science*, vol. 94, no. 1, pp. 213–219, 2019.
- [15] D. Rosenberg, L. Groussin, E. Jullian, K. Perlemino, X. Bertagna, and J. Bertherat, "Role of the PKA-regulated transcription factor CREB in development and tumorigenesis of endocrine tissues," *Annals of the New York Academy of Sciences*, vol. 968, no. 1, pp. 65–74, 2002.
- [16] I. Yajima, M. Y. Kumasaka, N. D. Thang et al., "Molecular network associated with MITF in skin melanoma development and progression," *Journal of skin cancer*, vol. 2011, Article ID 730170, 7 pages, 2011.
- [17] A. Kawakami and D. E. Fisher, "The master role of microphthalmia-associated transcription factor in melanocyte and melanoma biology," *Laboratory Investigation*, vol. 97, no. 6, pp. 649–656, 2017.
- [18] M. Kim, Y. Moon, J. C. Tou, B. Mou, and N. L. Waterland, "Nutritional value, bioactive compounds and health benefits of lettuce (*Lactuca sativa* L.)," *Journal of Food Composition and Analysis*, vol. 49, pp. 19–34, 2016.
- [19] B. Mou, "Handbook of plant breeding," in *Vegetables I: Asteraceae, Brassicaceae, Chenopodiaceae, and Cucurbitaceae*, J. Lettuce Prohens and F. Nuez, Eds., Springer, New York, NY, USA, 2008.
- [20] M. Kadam, V. Rajenimbalkar, A. Patil, and B. Bade, "Performance of promising lettuce variety Phule Padma (GKL-2) under Pune conditions," *International Journal of Farm Sciences*, vol. 12, no. 1, pp. 12–15, 2022.
- [21] A. Lafta, G. Sandoya, and B. Mou, "Genetic variation and genotype by environment interaction for heat tolerance in crisphead lettuce," *HortScience*, vol. 56, no. 2, pp. 126–135, 2021.
- [22] S. W. Jang, Y.-D. Kim, S. Lee, and S.-H. Yim, "Assessment of antioxidant activities of Heuknarang a novel Korean *Lactuca sativa* L.," *Food Science and Technology*, vol. 42, Article ID e06522, 2022.
- [23] Y. Ahn, H. H. Lee, B.-H. Kim et al., "Heukharang lettuce (*Lactuca sativa* L.) leaf extract displays sleep-promoting effects through GABAA receptor," *Journal of Ethnopharmacology*, vol. 314, Article ID 116602, 2023.
- [24] T. A. Bischoff, C. J. Kelley, Y. Karchesy, M. Laurantos, P. Nguyen-Dinh, and A. G. Arefi, "Antimalarial activity of lactucin and lactucopicrin: sesquiterpene lactones isolated from *Cichorium intybus* L.," *Journal of Ethnopharmacology*, vol. 95, no. 2-3, pp. 455–457, 2004.
- [25] X. Wang, M. Liu, G. H. Cai et al., "A potential nutraceutical candidate lactucin inhibits adipogenesis through down-regulation of JAK2/STAT3 signaling pathway-mediated mitotic clonal expansion," *Cells*, vol. 9, no. 2, p. 331, 2020.
- [26] M. K. Rasmussen and B. Ekstrand, "Regulation of 3β -hydroxysteroid dehydrogenase and sulphotransferase 2A1 gene expression in primary porcine hepatocytes by selected sex-steroids and plant secondary metabolites from chicory (*Cichorium intybus* L.) and wormwood (*Artemisia* sp.)," *Gene*, vol. 536, no. 1, pp. 53–58, 2014.
- [27] F. H. Zhang, Y.-L. Yan, Y. Wang, and Z. Liu, "Lactucin induces potent anti-cancer effects in HL-60 human leukemia cancer cells by inducing apoptosis and sub-G1 cell cycle arrest," *Bangladesh Journal of Pharmacology*, vol. 11, no. 2, pp. 478–484, 2016.
- [28] R. L. F. Amaral, M. Miranda, P. D. Marcato, and K. Swiech, "Comparative analysis of 3D bladder tumor spheroids obtained by forced floating and hanging drop methods for drug screening," *Frontiers in Physiology*, vol. 8, p. 605, 2017.
- [29] S. Chung, G. J. Lim, and J. Y. Lee, "Quantitative analysis of melanin content in a three-dimensional melanoma cell culture," *Scientific Reports*, vol. 9, no. 1, p. 780, 2019.
- [30] S.-H. Baek, J.-W. Ahn, S.-H. Nam, C.-S. Yoon, J.-C. Shin, and S.-H. Lee, "S-(–)-10, 11-dihydroxyfarnesoic acid methyl ester inhibits melanin synthesis in murine melanocyte cells," *International Journal of Molecular Sciences*, vol. 15, no. 7, pp. 12750–12763, 2014.
- [31] F. Pintus, D. Spano, A. Corona, and R. Medda, "Anti-tyrosinase activity of *Euphorbia characias* extracts," *PeerJ*, vol. 3, Article ID e1305, 2015.
- [32] C.-O. Chan, X.-J. Xie, S.-W. Wan et al., "Qualitative and quantitative analysis of sesquiterpene lactones in *Centipeda minima* by UPLC–Orbitrap–MS & UPLC–QQQ–MS," *Journal of Pharmaceutical and Biomedical Analysis*, vol. 174, pp. 360–366, 2019.
- [33] S. W. Jang, S.-H. Yim, and S. Lee, "Breeding of high functional ingredients lettuce 'Heukharang,'" *Korean Journal of Breeding Science*, vol. 54, no. 3, pp. 234–237, 2022.
- [34] A. Chairprasongsuk, T. Onkoksoong, T. Pluemsamran, S. Limsaengurai, and U. Panich, "Photoprotection by dietary phenolics against melanogenesis induced by UVA through Nrf2-dependent antioxidant responses," *Redox Biology*, vol. 8, pp. 79–90, 2016.
- [35] A. Di Petrillo, A. M. González-Paramás, B. Era et al., "Tyrosinase inhibition and antioxidant properties of *Asphodelus microcarpus* extracts," *Biomedical, Central Complementary and Alternative Medicine*, vol. 16, no. 1, pp. 453–459, 2016.
- [36] S.-C. Ko and S.-H. Lee, "Protocatechuic aldehyde inhibits α -MSH-induced melanogenesis in B16F10 melanoma cells via PKA/CREB-associated MITF downregulation," *International Journal of Molecular Sciences*, vol. 22, no. 8, p. 3861, 2021.
- [37] G.-E. Costin and V. J. Hearing, "Human skin pigmentation: melanocytes modulate skin color in response to stress," *The Federation of American Societies for Experimental Biology Journal*, vol. 21, no. 4, pp. 976–994, 2007.

- [38] C. Levy, M. Khaled, and D. E. Fisher, "MITF: master regulator of melanocyte development and melanoma oncogene," *Trends in Molecular Medicine*, vol. 12, no. 9, pp. 406–414, 2006.
- [39] N. Bentley, T. Eisen, and C. Goding, "Melanocyte-specific expression of the human tyrosinase promoter: activation by the microphthalmia gene product and role of the initiator," *Molecular and Cellular Biology*, vol. 14, no. 12, pp. 7996–8006, 1994.
- [40] C. Bertolotto, R. Buscà, P. Abbe et al., "Different cis-acting elements are involved in the regulation of TRP1 and TRP2 promoter activities by cyclic AMP: pivotal role of M boxes (GTCATGTGCT) and of microphthalmia," *Molecular and Cellular Biology*, vol. 18, no. 2, pp. 694–702, 1998.
- [41] H.-C. Huang, S.-J. Chang, C.-Y. Wu, H.-J. Ke, and T.-M. Chang, "[6]-Shogaol Inhibits α -MSH-Induced melanogenesis through the acceleration of ERK and PI3K/Akt-mediated MITF degradation," *Biomedical Research International*, vol. 2014, Article ID 842569, 9 pages, 2014.
- [42] Y. Kim, S. Cho, and Y. Seo, "The activation of melanogenesis by p-CREB and MITF signaling with extremely low-frequency electromagnetic fields on B16F10 melanoma," *Life Sciences*, vol. 162, pp. 25–32, 2016.
- [43] A. M. Ferreira, A. A. de Souza, R. D. C. R. Koga et al., "Anti-melanogenic potential of natural and synthetic substances: application in zebrafish model," *Molecules*, vol. 28, no. 3, p. 1053, 2023.